Characterization and Evaluation of Nanoparticle Release during the Synthesis of Single-Walled and Multiwalled Carbon Nanotubes by Chemical Vapor Deposition

SU-JUNG (CANDACE) TSAI,*,†
MARIO HOFMANN,‡ MARILYN HALLOCK,§
EARL ADA,‖ JING KONG,‡ AND
MICHAEL ELLENBECKER†

NSF Center for High-rate Nanomanufacturing (CHN), University of Massachusetts Lowell, One University Avenue, Lowell, Massachusetts 01854, Department of Electrical Engineering and Computer Science, Massachusetts Institute of Technology, Cambridge, Massachusetts 02139, Department of Environment, Health and Safety, Massachusetts Institute of Technology, Cambridge, Massachusetts 02139, and Campus Materials Characterization Laboratory, University of Massachusetts Lowell, One University Avenue, Lowell Massachusetts 01854

Airborne nanoparticles released during the synthesis of single-walled and multi-walled carbon nanotubes were measured and characterized. This study reported the field measurements during the development of carbon nanotube production. Monitoring data were taken and the sampling methods to characterize aerosol release were developed along with the modification of carbon nanotube production in a time period from 2006 to 2009. Particle number concentrations for diameters from 5 nm to 20 μm were measured using the fast mobility particle sizer and the aerodynamic particle sizer; the particles released from the furnace were found to be less than 500 nm in diameter. The morphology and elemental composition of the released nanoparticles were characterized by scanning and transmission electron microscopy and energy dispersive spectroscopy. Different operating conditions of multi-walled carbon nanotubes (MWCNT) production were studied to evaluate their effects on the number and morphology of aerosol particles, and the number of particles released. Carbon nanotube filaments and carbon particles in clusters were found among the released aerosol particles during production of multiwalled carbon nanotubes.

Introduction

The field of nanotechnology has progressed rapidly in the two decades since the carbon nanotube (CNT) was discovered (*1*). Nanotechnology refers to the productive use of materials on the nanometer size scale. It is generally agreed that a "nanoparticle" is a particle with at least one dimension less than 100 nm (*2*). Carbon nanotubes, fibers with dimensions of a few to tens of nanometers, meet this definition. In this paper, nanoparticle is used when referring to nanoparticles in general, while "CNT" refers specifically to carbon nanotubes. CNTs are now being manufactured in large quantities, and many uses are being investigated; this widespread interest, however, has brought increased attention to research into toxicity, human exposure, and environmental releases associated with CNT manufacture and use.

Emissions from CNT furnaces have not been extensively characterized. CNT synthesis by chemical vapor deposition (CVD) is very inefficient: less than 3% of carbon feedstock is actually converted to CNTs (*3*). As small furnaces in universities are scaled up to production levels in industry, there is increasing concern regarding emissions to the environment. In January 2009 the state of California asked all manufacturers of CNTs to submit information on CNT operations and release from their facilities, including fate and transport in the environment. The environmental fate and transport of engineered nanoparticles, including CNTs, has been a subject of increasing concern in recent years (*4, 5*).

The toxicity testing of CNT has been limited to date. Early studies tested CNTs in short-term single dose assays of pulmonary toxicity by instilling or aspirating CNTs into mice and rat lungs. In general these studies found inflammation and granulomas comparable to the toxic dust quartz (*6, 7*). However, Shvedova et al. (*8, 9*), in both a single-dose aspiration study and a four-day inhalation study, found an initial inflammatory response followed by granulomas, fibrosis, and decreased rates of respiration and bacterial clearance from the lungs. Two recent studies found asbestos-like effects in short-term bioassays when CNTs were injected intraperitoneally into mice (*10, 11*).

There are many aspects of these first toxicology studies, beyond the usual difficulties inherent in any toxicology study of inferring human toxicity from animal data, that limit their direct applicability to human exposure. These issues are reviewed in some detail by Warheit (*12*). The term "carbon nanotube" does not define a single entity, in the way that "silica particle" does. There are many different CNT: single-walled and multi-walled, different catalysts, "dirty" vs purified, long vs short, etc. Each toxicology study used either single-walled CNTs (*6–9*) or multiwalled CNTs (*10, 11*), thus limiting the generalizability of the results. In addition, most of the published studies did not use CNT inhalation to deliver the dose; typically, a single dose was delivered via intratracheal instillation (*6, 7*), aspiration (*8*), or intraperitoneal injection (*10, 11*). The only study that used inhalation was Shvedova et al. (*9*); similar but more severe toxicological responses were found when inhalation was used rather than aspiration.

In order to maximize the possible response, the single doses used are extremely large compared to any possible occupational or environmental exposure. For example, Shvedova et al. (*8*) exposed mice to single doses of single-walled CNTs via aspiration; the highest dose was 40 mg; assuming that a "typical" single-walled CNT can be modeled by a solid carbon cylinder 10 nm in diameter by 10 μm long, this is equivalent to 2×10^{12} CNTs. If a worker were exposed to 1 CNT/cm^3 (see exposure discussion below), (s)he would inhale approximately 10^7 CNTs in the course of one workday; the dose used in the NIOSH study thus would represent hundreds of years of occupational exposure.

* Corresponding author phone: 1-978-934-4366; fax: 1-978-934-3050; e-mail: SuJung_Tsai@uml.edu.
† NSF Center for High-rate Nanomanufacturing (CHN).
‡ Department of Electrical Engineering and Computer Science, Massachusetts Institute of Technology.
§ Department of Environment, Health and Safety, Massachusetts Institute of Technology.
‖ Campus Materials Characterization Laboratory.

In spite of the recognized shortcomings in the published CNT toxicology studies, there appears to be sufficient evidence for concern. Shvedova et al. (8) exposed mice to the same doses of CNTs and silica, a known fibrinogen; the CNT-exposed mice developed fibrosis, while the silica-exposed mice did not. The studies finding a possible association between CNT exposure and mesothelioma are of particular concern, since mesothelioma is a deadly disease associated historically with exposure to asbestos (13). Because of the cancer risk, the OSHA 8 h time-weighted average permissible exposure limit for asbestos is only 0.1 fiber/cm^3 (14).

Because of concerns about potential toxicity, measurements of release and exposure to CNTs are needed. There have been few published studies of CNT exposure in the workplace; Maynard et al. (15) found almost no release of fibers when CNT were removed from a high pressure carbon monoxide reactor and transferred into a secondary container. The peak mass concentration measured during the transfer procedure was low (53 μg/m^3). Han et al. (16) conducted air monitoring for MWCNTs during several procedures in a research laboratory. They found that levels of MWCNTs during a blending procedure generated MWCNT concentrations between 172.9 and 193.6 CNT/cm^3. The addition of an enclosure and exhaust ventilation reduced levels to between 0.018 and 0.05 CNT/cm^3.

In summary, previous studies regarding exposure to CNTs showed almost no release to the workplace during the production process, provided that the processes were adequately enclosed and vented. Airborne concentrations were measured at room background locations during the monitored operations. The morphology and quantity of aerosols found in furnace exhaust during the synthesis of carbon nanotubes and possibly emitted to the environment have not been reported to date and the effect of operating conditions has not been studied. Operating conditions significantly change the growth mechanism (17).

This study was conducted as field monitoring in the time period of 2006 to 2009 during the development of carbon nanotube production, thus, the sampling method was developing along with modification of production from single-walled to multiwalled CNT to determine a successful sampling method and investigate the environmental release. The study reported here investigated the effect of different operating conditions on the number and morphology of aerosol particles released from a CVD furnace. These results should contribute to further development of strategies for the evaluation and control of CNT environmental release and human exposure.

Materials and Methods

Experimental Process. This research was conducted in two parts, i.e., evaluations of the synthesis of SWCNTs, performed in 2006 and MWCNTs, a new development performed in 2009. SWCNTs are normally produced with a prepatterned catalyst; in order to determine the effect of the catalyst on aerosol production, the experiment was repeated without the catalyst present. The evaluation of MWCNT production through continuous catalyst injection was performed for two scenarios; i.e., growing MWCNTs on a substrate, and having no substrate for the growth. For the no substrate scenario, two different conditions, high and low injector temperature, were tested to evaluate the effect of temperature on released nanoparticles during synthesis. A list of experiments and notation used is provided in Supporting Information (SI) Table S1.

All experiments were performed in a common laboratory CVD setup consisting of a 2.5 × 60 cm fused silica cylindrical reactor chamber heated by a clamshell furnace located in a laboratory fume hood. To produce SWCNTs, substrate-bound
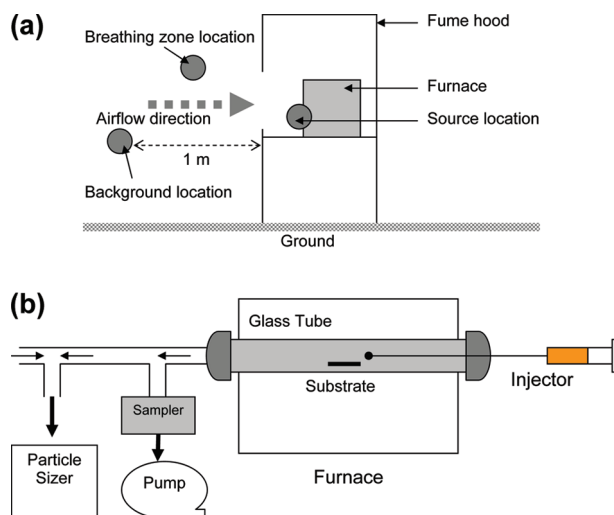
FIGURE 1. (a) Illustration of measuring locations (b) Illustration of process diagram.

SWCNTs were obtained by depositing a catalyst on a Si/SiO$_2$ substrate prior to synthesis. The sample was then pretreated as previously described (11) and CNT were grown for 20 min at 925 °C with ethanol as the carbon feedstock in a stream of 600 scm^3/min Ar and 440 scm^3/min H$_2$. The resulting CNT are expected to be firmly attached to the substrate at one point at their upstream end and with the other end floating several hundreds of micrometers over the substrate during synthesis (18). Once they make contact with the substrate, strong van der Waals interaction keeps them attached over the whole length of the sample. SI Figure S1a is a scanning electron microscope (SEM) image which demonstrates that the obtained CNT are aligned in a parallel manner by the gas flow and at least several hundred micrometers long. Aerosol-assisted CVD was used to generate MWCNTs at high yield following the procedure of Xiang et al. (19). In this approach both the catalyst and the carbon feedstock were continuously introduced into the reaction zone during the 20 min CVD process by evaporating a solution of ferrocene and cyclohexane at a feeding rate of 10 mL/h from a heated nozzle. The resulting CNTs grew on the reactor walls and Si/SiO$_2$ substrates and exhibit a forest-like alignment as shown in SI Figure S1b. Varying the temperature of the injector nozzle affected the morphology of the obtained nanotube films; at a low nozzle temperature of ∼100° MWCNT forest-like structures of 600 μm height were synthesized whereas increasing the nozzle temperature resulted in carpet-like structures. The reaction temperature was 800 °C which is substantially lower than for the SWCNT growth and a gas stream of 500 scm^3/min Ar and 50 scm^3/min H$_2$ were used. The difference in growth protocol is related to different applications of these materials. The SWCNTs were generated from a predefined catalyst area for applications in electronic devices, where low density and flow alignment are required. The continuous introduction of catalyst and carbon feedstock in the case of MWCNT growth creates high density films for structural applications.

Monitoring and Sampling Procedure. Fast mobility particle sizer (FMPS) and aerodynamic particle sizer (APS) were used to monitor particle release. Equipment use is described in the SI. Measurements were taken at the background, breathing zone and source locations as illustrated in Figure 1a, notation listed in the SI. Background particle concentration was measured 1 m from the fume hood to represent the concentration in the room. The breathing zone concentration was measured in the researcher's working area which is about 0.5 m from the hood. Also shown is the sampling location of the FMPS and APS at the
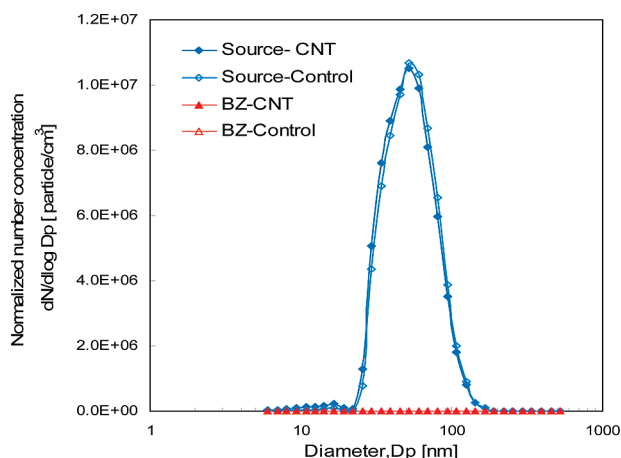
FIGURE 2. Particles number concentration during synthesis of SWCNT at the source and the background locations.

FIGURE 3. Particle number concentration and size distribution at source location. L-temp A: Low temperature, use substrate; L-temp B: Low temperature, no substrate; H-temp B: High temperature, no substrate.

particle release source, designated the source location, which was inside the fume hood. The source location was defined as the exhaust of the reactor inside the fume hood. Since the exhaust gas flow (2 L/min) was less than the required FMPS (10 L/min) and APS (5 L/min) sample air flow, the incoming exhaust stream was diluted with air from the fume hood as shown in Figure 1b. The measurements by FMPS and APS were taken individually. The exhaust from the SWCNT reactor went through a water bath placed inside the fume hood under normal operations. The water bath was not used for these experiments in order to measure actual particles released from the furnace. For MWCNT synthesis, the exhaust normally went through a cellulose acetate filter, which also was not used for these experiments. Background concentration in the room was recorded before, during, and after each operation. Source concentration was recorded before and during the synthesis of CNT.

The FMPS and APS measurements yield detailed information about airborne particle size distribution, but give no information about particle morphology and elemental composition. To provide this information, aerosol particles were collected for analysis. For SWCNT production, the sampling method is described in the SI. For MWCNT production, a new nanoparticle aerosol filter sampler (*20*) was used in these experiments. The sampling location is shown in Figure 1b. A schematic layout of the sampling device is shown in SI Figure S2. Transmission electron microscope (TEM)-copper grids (SPI 400 mesh with a Formvar/carbon film) were taped onto 47 mm diameter polycarbonate membrane filters (0.2 μm pore size). Fiber backing filters were used to support the polycarbonate filters. Air was drawn through the filters at 0.3 L/min using a calibrated personal sampling pump, and aerosol particles deposited on the grid via Brownian diffusion. This deposition process has been confirmed both experimentally and theoretically, as described in the SI.

Analytical methods are described in the SI.

Results

Results for SWCNT Production. Typical results of the aerosol monitoring at the exhaust from the reactor during SWCNT production are shown in Figure 2. Only FMPS data are shown in Figure 2, since the APS was not available at the time of the measurements. Measurements were taken under two conditions, i.e., the experimental data were obtained during SWCNT growth using a catalyst and the control data were obtained without a catalyst which results in no production of nanotubes during the furnace operation. As shown in Figure 2, particle concentrations measured at the source location peaked at a dimension of approximately 50 nm and
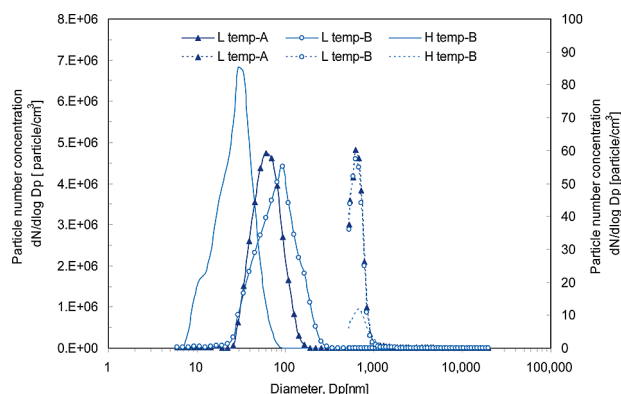
were as high as 10^7 particles/cm^3, close to the maximum concentration measurable by the FMPS. The exposure concentrations measured at the breathing zone location (designated as "BZ" in Figure 2) outside the fume hood were less than 2000 particles/cm^3. This indicates that the nanoparticles released from the furnace did not escape from the fume hood, and the fume hood sufficiently removed released nanoparticle during SWCNT synthesis. In addition, the exposure concentration at the background location was low prior to the experiment due to the effective general ventilation system designed for the new laboratory that could maintain the low background laboratory concentration of less than 2000 particles/cm^3. The difference between the particle total number concentration at the source and breathing zone was greater than 10^6 particles/cm^3. The difference between particle concentrations during SWCNT growth and the control experiments is small, which could be due to conditioning effects in CVD reactors that were used prior to these experiments, i.e., despite the absence of catalyst on the substrate, the catalytic activity of the reactor walls seems to be sufficient to generate carbon nanoparticles in the gas stream. The mechanism that produced nanoparticles at such high concentrations during production is not clear. This conditioning effect is still subject to investigation but seems to be related to the presence of catalyst that deposited on the reactor walls. Before every growth the reactor was oxidized at 1000 °C in an attempt to passivate these catalyst particles and ensure that no carbon particulates were present. The results of particle sampling are available in the SI.

Results for MWCNT Production. *Comparison of Particle Concentrations at Different Locations.* Typical results of the aerosol concentration measurements at the furnace exhaust during synthesis of MWCNTs are shown in Figures 3 (furnace exhaust), SI Figure S4 (room background), and SI Table S2. The background concentrations in the nanoparticle size range were all very low compared to those at the source, as shown in SI Table S2. The monitoring in the case of high injector temperature using substrate was not performed because it resulted in a low production yield, thus this condition was not of interest for the manufacturing process. The particle concentrations measured at the source and the background location are plotted in Figure 3 and SI Figure S4 respectively; the primary *y*-axis on the left is the scale for particle concentrations in the complete size range (5−20 000 nm) which are shown by the solid line curves; the secondary *y*-axis on the right is the scale for particle concentrations for the larger size range of 550−20 000 nm which are shown by the dotted line curves. The released particles at the source during synthesis were found to be at a high concentration (Figure 3), more than 4×10^6 particles/cm^3; the concentrations at the background, however, were low and close to the baseline

(SI Figure S4). The released particle size distributions varied by the operating condition, but most particles were less than 300 nm in diameter. Due to scale differences between the two vertical axes in Figure 3, the performance of the two instruments at the common measurement point of 500 nm cannot be compared. The actual data, however, were similar, with a measured concentration on both instruments of approximately 50 particles/cm^3 at a diameter of 500 nm. The particle concentrations and size distribution in the range above 550 nm were very similar at the source and the background, indicating that no aerosol particles above one-half micrometer in diameter were released at the source during synthesis.

The total particle concentrations for the measurements plotted in Figure 3 and SI Figure S4 are shown in SI Table S2. The numbers in Table S2 are the actual FMPS and APS data. These data were affected by two experimental conditions. First, approximately 15% of the furnace exhaust was diverted to the filter sample, so that the number of particles reaching the FMPS and APS was reduced by this fraction. Second, the furnace air was diluted with room air at a rate of approximately 4 to 1 and 5 to 2 for FMPS and APS, respectively; so the actual furnace concentrations would have been higher than the values reported in SI Table S2 by the same factors. Thus, the values in Table S2 only reflect relative particle concentrations under different conditions, not absolute ones. The size distributions shown in Figure 5 and SI Figure S2 are not affected by the dilution. The total concentrations of particles at the source for sizes less than 560 nm were about $2-3 \times 10^6$ particles/cm^3, and the concentrations at the background were extremely low compared to the source. The total concentrations for particle sizes >500 nm at both the source and background are very similar as seen in Figure 3 and SI Figure S4. Background levels outside the fume hood during synthesis were identical to background levels before processing began, indicating no release of particles from the hood.

Comparison of Substrate Presence and Temperature. Three conditions were evaluated while measuring particle release during synthesis of MWCNTs. For MWCNT production, in the case of low injector temperature, two scenarios were chosen. In the first scenario (L-temp A) a substrate was placed inside the reaction chamber to collect the CNT during growth, and in the second scenario (L-temp B) no substrate for MWCNT growth was used. For the case of high injector temperature (H-temp B), no substrate was used. The quantity and size of particles below 550 nm that were released during synthesis was affected by the operating conditions described above, as shown in Figure 3 and SI Figure S4. Particles released at the source when using a substrate was used for MWCNT growth were in the size range of $25-100$ nm with the particle mode at 60 nm as shown by the solid curve "L temp-A" in Figure 3. The solid curve "L temp-B" represents the particle release at the source when the substrate was not present. The particles released during synthesis without using a substrate yielded a similar but broader particle size distribution from 20 to 200 nm with a larger particle mode at about 95 nm as shown on the solid curve "L temp-B" in Figure 3.

The variation in temperature of the injector needle resulted in significant differences in the particle concentration and size distribution of released particles at the source as seen on the solid curves "L temp-B" and "H temp-B" in Figure 3. Particles released at the high temperature condition were in a smaller size range of $7-90$ nm compared to the particles released at low temperature condition with a size range of $20-200$ nm. In addition, the highest particle concentration measured at the high temperature condition approached 7×10^6 particles/cm^3. The particle concentration above 500 nm size showed a much lower value of 10 particles/cm^3 peaking at 700 nm at the condition of high injector tem-

perature compared to the other conditions. However, the total concentrations at the source and the background locations are similar in all cases for particles above 500 nm.

Characterization of Aerosol Particles by TEM. For MWCNT production, particles released in the exhaust were collected using the aerosol filter sampler. The particles collected on grids under the different operating conditions were characterized by TEM as shown in Figure 4. For low-temperature injector conditions, the particle concentration was higher during no-substrate synthesis as shown in Figure 3 and SI Table S2, and indeed the TEM images showed a higher density as can be seen in Figures 4a and 4b. In addition, for the low injector temperature the collected particles were predominantly clusters of spherical shape with some individual nanoparticles, as well as MWCNTs. The individual spherical nanoparticles are as small as 20 nm, and the size of clusters have a broader distribution but are no larger than 300 nm as can be seen in Figure 4a and 4b. This result is consistent with the measurement of particle concentration shown in Figure 3.

CNT filaments were found among the aerosol particles collected when applying high injector temperature during synthesis as seen in Figure 4c, e, and f. The morphology of particles produced at the different injector temperatures is shown in Figure 4c and d: A multitude of CNT filaments attached to clusters of nanoparticles was collected. The filaments are few nanometers in diameter, as seen in Figure 4e and f and are from few nanometers to several micrometers in length. Our TEM method was designed to identify particle morphology and elemental analysis. Particles were not counted on the TEM grids, since this is very labor-intensive and the particle count distribution is obtained from the FMPS and APS.

Elemental analysis was performed on typical clusters of light and dark gray individual nanoparticles (marked by arrows) that were collected at both high and low injector temperature; an example is indicated by the circle in Figure 4f. The results of the elemental analysis are shown in SI Figure S5. While the Cu peaks and some contribution to the C and O peaks are expected to originate from the TEM grid, the Fe peaks are due to the collected particles and are likely from the dark gray particles which seem to include the Fe catalyst. This indicates that the particles are both clusters of carbon particles and iron catalyst particles coated with carbon.

Samples of MWCNTs synthesized at the low injector temperature were collected by scraping MWCNTs from the substrate. Grids were gently contacted to the MWCNTs and the attached MWCNTs were analyzed by TEM; the collected nanotubes are about 50 nm in diameter as can be seen in images of SI Figure S6a and b. In SI Figure S6b, the multiple layers inside a MWCNT can be seen at a fracture site of a nanotube.

Particle Concentration Change for The Laboratory Background. Particle concentrations at the laboratory background were measured before, during and after synthesis of CNT. The purpose was to evaluate the extent of particle release from the fume hood to the room. Typical measurements taken when using the low injector temperature for synthesis are shown in SI Figure S7, which shows the actual number concentration in the room. The concentration changes before furnace operation (no symbol line) and during operation (symbol line) varied by particle size, and the distribution patterns were similar. The consistent particle distribution pattern indicates that the concentration changes were due to the variability of the general ventilation system in the laboratory, and not associated with nanoparticles released from furnace. It should not be assumed that the excellent protection afforded by the fume hood used here would be provided by every chemical fume hood. A study by Tsai et al. (20)
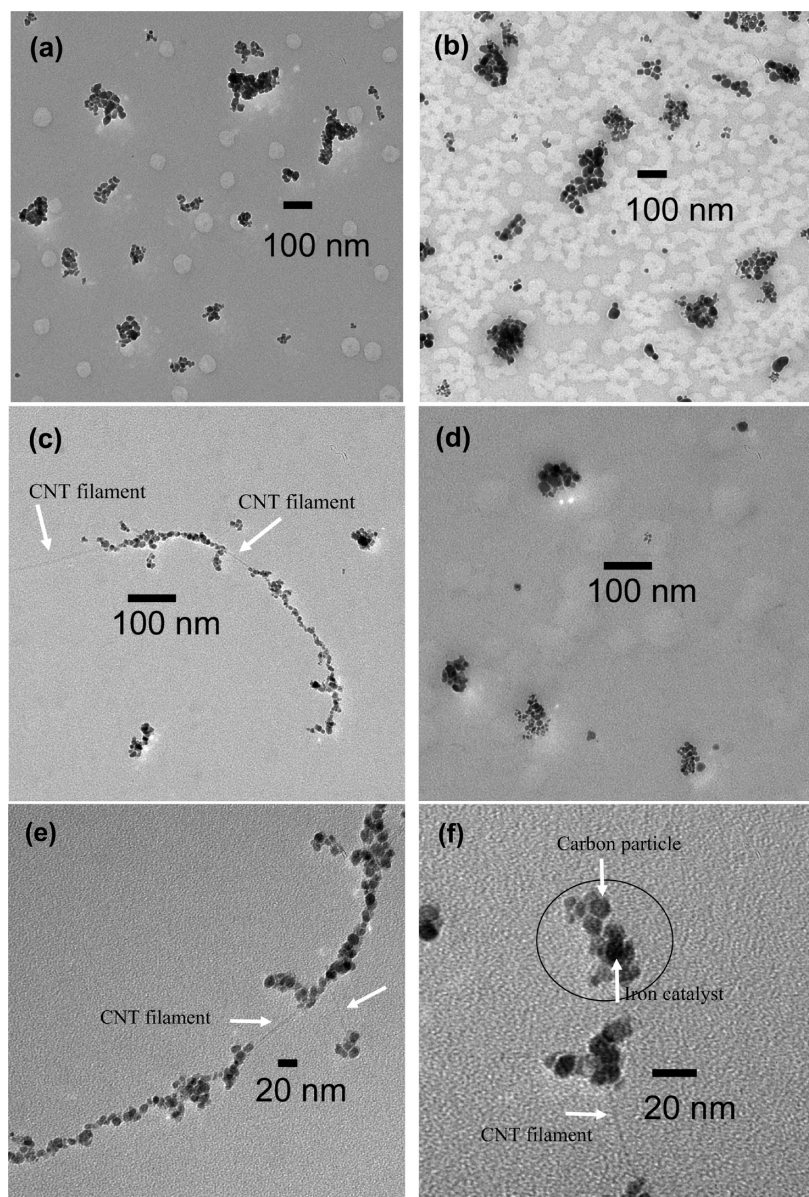
FIGURE 4. TEM images of collected aerosol particles from different conditions of MWCNT production (a) L temp-A, Direct Mag:15 600× (b), L temp-B, Direct Mag:15 600×, (c) H temp-B, Direct Mag:26 000×, (d) L temp-B, Direct Mag:26 000×, (e) and (f) TEM images of MWCNT filaments collected from condition of high injector temperature and no substrate use (H temp-B).

found significant nanoparticle release associated with handling nanopowder when using a traditional conventional fume hood. Tsai's study found that the use of a conventional hood could result in a more intense exposure to workers using the hood, due to a complex circulating airflow pattern between the worker and the hood. However, detectable quantities of nanoparticles were not released into the room when using this particular fume hood during the furnace operation. This is likely due to certain favorable factors of the design and operation. The furnace was operated in an extra wide (1.6 m width × 0.76 m height) constant velocity fume hood, the sash was set at a 40 cm height location (0.7 m/s face velocity) during the whole operating process, and no worker was present at the hood face. A wider hood, intermediate face velocity, and no worker standing in front of the hood can minimize the generation of turbulent airflow at the hood face, which could explain the good performance when using this hood.

Discussion

The evaluation of the SWCNT production found that aerosol nanoparticles released during synthesis were detected at the source by the FMPS; however, sampled particles could not be individually identified for analysis. The production scale of ultralong SWCNTs was limited to a few micrograms per operation which made the collection of released SWCNTs difficult. In addition, catalyst was deposited on the surface of the silicon substrate and SWCNTs are not expected to be released during the synthesis process. The morphology of the released nanoparticles from SWCNT synthesis could therefore not be characterized from this study. The measurements from the FMPS found that the released airborne nanoparticles were all less than 100 nm and were released at a high particle concentration. These particles are likely to be carbonaceous byproduct from the CVD synthesis process.

Due to the larger amounts of precursors, a greater quantity of aerosol nanoparticles was released during synthesis of MWCNTs. For the MWCNT production, the injector temperature had a substantial effect on the particle size distribution; this is likely due to the dispersion process of the catalyst solution, since at high temperatures the evaporation of the catalyst is faster. The subsequent formation at higher temperatures of small clusters from an environment of gasified precursor will result in fine filaments which can travel through the reactor without depositing on its walls.

When the liquid catalyst is introduced at low temperature the droplets will not evaporate completely but form large particles. These particles cannot act as initiators for nanotube growth because of their size and they will only be coated with carbon instead of precipitating a nanotube. However, when deposited on the reactor walls they can decrease their diameter by evaporation and initiate substrate-bound growth. In other words, MWCNTs were well formed and attached on the substrate under low injector temperature operation. High injector temperature reduced the growth of MWCNTs on the substrate; instead, filaments were formed in the air and were released in the furnace exhaust. Thus, a low injection temperature has the double advantage of increasing MWCNT production while decreasing environmental release of nanoparticles as can be seen by the particle concentration shown in Figure 3.

The use of a substrate for MWCNT production results in fewer nanoparticles released into the air because the increased surface area can afford more CNTs growing inside the reactor instead of being released in the exhaust. Consequently, a higher yield production for growing MWCNT on substrate could reduce the formation of aerosol filaments. However, the magnitude of nanoparticle release during all production conditions tested was very high with particle concentration usually exceeding 10^6 particles/cm^3 at the source. Several reports have studied the toxicity of CNT, while the toxicity of carbon nanoparticles containing an iron catalyst, found to be released in this study, is unknown. The formation of filaments could be minimized while enhancing production by optimizing process conditions, but carbon particles were still formed in high quantity. The environmental release could cause certain impacts on human health and the environment when the reactor exhaust is released directly into the air. For the normal operation of this process, the exhaust tube was filtered through a cellulose acetate filter and then through a water bath to prevent reverse airflow into the reactor; this had the added advantage that some aerosol particles in the exhaust air were captured in the water. The capture efficiency of the water bath is not known, however, and is likely to be fairly low. Consequently, further research to investigate more efficient methods of nanoparticle control for the furnace exhaust was designed as a follow-up to this study.

Release of airborne nanoparticles was not detectable at the laboratory background location for all operations. This indicates that the capture of nanoparticles released from the furnace by the fume hood was efficient during these experiments. However, research has demonstrated that nanoparticles can be released from fume hoods under some circumstances, e.g., increased circulation of airflow between researchers and the hood (21−23) and inappropriate hood face velocity (20). In conclusion, the operation of a CNT furnace in a well-designed ventilation hood or other ventilated enclosure is essential to prevent exposure of researchers to nanoparticles during CNT synthesis.

Supporting Information Available

Details of the equipment, sampling and analytical methods used, background sampling results, EDS results, and more useful information. This material is available free of charge via the Internet at http://pubs.acs.org.

Literature Cited

(1) Iijima, S. Helical microtubules of graphitic carbon. *Nature* **1991**, *354*, 56–58.

(2) Maynard, A. D.; Kuempel, E. D. Airborne nanostructured particles and occupational health. *J. Nanopart. Res.* **2005**, *7*, 587–614.

(3) Plata, D. L.; Hart, A. J.; Reddy, C. M.; Gschwend, P. M. Early evaluation of environmental impacts of carbon nanotube synthesis by catalytic chemical vapor deposition. *ACS Nano* **2009**, Submitted.

(4) Joner, E. J.; Hartnik, T.; Amundsen, C. E. Environmental Fate and Ecotoxicity of Engineered Nanoparticles, Report No. TA 2304/2007; Norwegian Pollution Control Authority: Oslo, 2008.

(5) *Nanoscience and Nanotechnology: Environmental and Health Impacts*; Grassian, V. H., Ed.; John Wiley and Sons: New York, 2008.

(6) Lam, C. W.; James, J. T.; McCluskey, R.; Hunter, R. L. Pulmonary toxicity of single-walled carbon nanotubes in mice 7 and 90 days after intratracheal instillation. *Toxicol. Sci.* **2004**, *77*, 126–134.

(7) Warheit, D. B.; Laurence, B. R.; Reed, K. L.; Roach, D. H.; Reynolds, G. A. M.; Webb, T. R. Comparative pulmonary toxicity assessment of single-wall carbon nanotubes in rats. *Toxicol. Sci.* **2004**, *77*, 117–125.

(8) Shvedova, A. A.; Kisin, E. R.; Mercer, R.; Murray, A. R.; Johnson, V. J.; Potapovich, A. I.; Tyurina, Y. Y.; Gorelik, O.; Arepalli, S.; Schwegler-Berry, D.; et al. Unusual inflammatory and fibrogenic pulmonary responses to single-walled carbon nanotubes in mice. *Am. J. Physiol. Lung Cell Mol. Physiol.* **2005**, *289*, L698–L708.

(9) Shvedova, A. A.; Kisin, E. R.; Murray, A. R.; Johnson, V. J.; Gorelik, O.; Arepalli, S.; Hubbs, A. F.; Mercer, R.; Keohavong, P.; Sussman, N.; et al. Inhalation vs. aspiration of single-walled carbon nanotubes in C57/BL6 mice: inflammation, fibrosis, oxidative stress, and mutagenesis. *Am. J. Physicol. Lung Cell Mol. Physiol.* **2008**, *295*, L552–L565.

(10) Takagi, A.; Hirose, A.; Nishimura, T.; Fukumori, N.; Ogata, A.; Ohashi, N.; Kitajima, S.; Kanno, J. Induction of mesothelioma in p53± mouse by intraperitoneal application of multi-wall carbon nanotube. *J. Toxicol. Sci.* **2008**, *33*, 105–116.

(11) Poland, C. A.; Duffin, R.; Kinloch, I.; Maynard, A.; Wallace, W. A. H.; Seaton, A.; Stone, V.; Brown, S.; MacNee, W.; Donaldson, K. Carbon nanotubes introduced into the abdominal cavity of mice show asbestos-like pathogenicity in a pilot study. *Nat. Nanotechnol.* **2008**, *3*, 423–428.

(12) Warheit, D. B. Nanoparticles: Health impacts? *Mater. Today* **2004**, http://www.materialstoday.com/pdfs_7_2/warheit.pdf.

(13) Wagner, J. C.; Sleggs, C. A.; Marchand, P. Diffuse pleural mesothelioma and asbestos exposure in the North Western Cape province. *Brit. J. Ind. Med.* **1960**, *17*, 260–271.

(14) U.S. Occupational Safety and Health Administration. *Table Z-1 Limits for Air Contaminants*, 29 CFR 1910.1000 Table Z-1; OSHA: Washington, DC, 2006.

(15) Maynard, A.; Baron, P. A.; Foley, M.; Shvedova, A. A.; Kisin, E. R.; Castranova, V. Exposure to carbon nanotube material: aerosol release during the handling of unrefined single walled carbon nanotube material. *J. Toxicol. Environ. Health.* **2004**, *67*, 87–107.

(16) Han, J. H.; Lee, E. J.; Lee, J. H.; So, K. P.; Lee, Y. H.; Bae, G. N.; Lee, S. B.; Ji, J. H.; Cho, M. H.; Yu, J. Monitoring multiwalled carbon nanotube exposure in carbon nanotube research facility. *Inhal. Toxicol.* **2008**, *20*, 741–749.

(17) Reina, A.; Hofmann, M.; Zhu, D.; Kong, J. Growth mechanism of long and horizontally aligned carbon nanotubes by chemical vapor deposition. *J. Phys. Chem. C* **2007**, *111* (20), 7292–7297.

(18) Hofmann, M.; Nezich, D.; Reina, A.; Kong, J. In-situ sample rotation as a tool to understand chemical vapor deposition

growth of long aligned carbon nanotubes. *Nano Lett.* **2008**, *8* (12), 4122–4127.

(19) Xiang, R.; Luo, G.; Qian, W.; Wang, Y.; Wei, F.; Li, Q. Large area growth of aligned CNT arrays on spheres: towards the large scale and continuous production. *Chem. Vap. Deposition* **2007**, *13* (10), 533–536.

(20) Tsai, S.; Ada, E.; Isaacs, J.; Ellenbecker, M. Airborne nanoparticle exposures associated with the manual handling of nanoalumina and nanosilver in fume hoods. *J. Nanopart. Res.* **2009**, *11* (1), 147–161.

(21) Kim, T. H.; Flynn, M. R. Airflow pattern around a worker in a uniform freestream. *Am. Ind. Hyg. Assoc. J.* **1991**, *52*, 287–296.

(22) Kim, T. H.; Flynn, M. R. Modeling a worker's exposure from a hand-held source in a uniform freestream. *Am. Ind. Hyg. Assoc. J.* **1991**, *52*, 458–463.

(23) Kim, T. H.; Flynn, M. R. The effect of contaminant source momentum on a worker's breathing zone concentration in a uniform freestream. *Am. Ind. Hyg. Assoc. J.* **1992**, *53*, 757–766.